

# Search for production of a Higgs boson and a single top quark in $\mu\mu$ final states in proton collisions at $\sqrt{s} = 13$ TeV

Departamento de Investigacion en Física  
Maestría en Ciencias (Física)  
Hiram Ernesto Damián

Universidad de Sonora

May 14, 2019



# Contenido

- 1 Overview and motivation
- 2 Higgs theory
- 3 tH mechanisms
- 4 Production cross section
- 5 Higgs Branching ratios
- 6 Fitting
- 7 Results
- 8 Conclusions
- 9 References
- 10 Supportive slides



## Overview

- Through this project we will investigate the production of Higgs boson in association with a single top quark ( $tH$ ) in proton-proton collisions with the CMS experiment of the LHC. This mechanism of production of the Higgs boson has not been observed before by any experiment.
  - Understanding the production of the Higgs boson, as well as its decays are an important part of the physical program of the CERN international laboratory experiments that try to complete the tests to verify the Standard Model, the theory of the fundamental particles



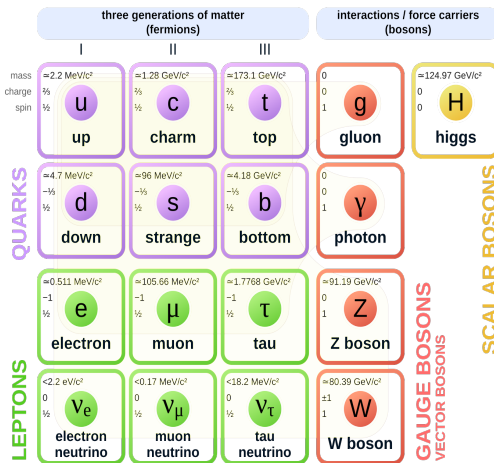
## Motivation for single top Higgs (tH)

- Coupling measurement is essential to establish the nature of the Higgs
  - The exploration of Higgs production on the tH channel is subject relatively new. Measurements of CMS and ATLAS are compatible with SM predictions.
  - The tH study explores the relative sign of top-Higgs and W-Higgs couplings.  
Small deviations from SM predictions could be associated with physics beyond the standard model (BSM) such as String Theory and Supersymmetry.



# Standard Model

## Standard Model of Elementary Particles



## Particles Properties

## Table of particles in SM

Particle	Mass ( $\text{MeV}/c^2$ )	Charge	spin	Lifetime (s)	Distance in lifetime (meters)
Up (u)	2.2	$\frac{2}{3}$	$\frac{1}{2}$	stable	-
Charm (c)	1280	$\frac{2}{3}$	$\frac{1}{2}$	$1.1 \times 10^{-12}$	$23.39 \times 10^{-4}$
Top (t)	173100	$\frac{2}{3}$	$\frac{1}{2}$	$5 \times 10^{-25}$	$1.06 \times 10^{-15}$
Down (d)	4.6	$-\frac{1}{3}$	$\frac{1}{2}$	Stable	-
Strange (s)	96	$-\frac{1}{3}$	$\frac{1}{2}$	$1.24 \times 10^{-8}$	26.37
Bottom (b)	4180	$-\frac{1}{3}$	$\frac{1}{2}$	$1.3 \times 10^{-12}$ s	$27.64 \times 10^{-4}$
W	80379	$\pm 1$	1	$3 \times 10^{-25}$	$6.37 \times 10^{-16}$
Z	91187.6	0	1	$3 \times 10^{-25}$	$6.37 \times 10^{-16}$
Photon ( $\gamma$ )	0	0	1	Stable	-
Gluon (g)	0	0	1	Stable	-
Higgs (H)	125.18	0	0	$1.56 \times 10^{-22}$	$3.31 \times 10^{-13}$
Electron (-e)	0.511	-1	$\frac{1}{2}$	Stable	-
Muon ( $\mu$ )	105.7	-1	$\frac{1}{2}$	$2.2 \times 10^{-6}$	4678.61
$\tau$	1776.86	-1	$\frac{1}{2}$	$2.9 \times 10^{-13}$	$61.67 \times 10^{-5}$
$\nu_e$ $\nu_\mu$ $\nu_\tau$	0	0	$\frac{1}{2}$	Stable	-



Stable means no decay, or lifetime almost infinite. Particles speeds at  $0.99c$

## Electroweak SM Lagrangian

The standard model is a theory of fields with spins 0,  $\frac{1}{2}$  and 1. The SM lagrangian

$$\mathcal{L} = \mathcal{L}_{\text{gauge}} + \mathcal{L}_f + \mathcal{L}_{\text{higgs}} + \mathcal{L}_{\text{yukawa}}$$

donde

- $\mathcal{L}_{\text{gauge}} = -\frac{1}{4} [F^{\mu\nu} F_{\mu\nu}] - \frac{1}{4} [G^{i\mu\nu} G^i_{\mu\nu}]$ 
    - $F^{\mu\nu} = \partial_\mu B_\nu - \partial_\nu B_\mu$
    - $G^{i\mu\nu} = \partial_\mu W_\nu^i - \partial_\nu W_\mu^i - g \epsilon^{ijk} W_\mu^j W_\nu^k$
  - $\mathcal{L}_f = i\bar{\Psi}_L \not{D} \Psi_L + i\bar{\psi}_R \not{D} \psi_R$  is the kinematic term for fermions
    - $D_\mu \Psi_L = (\partial_\mu + igW_\mu + ig'Y_L B_\mu) \Psi_L$
    - $D_\mu \psi_R = (\partial_\mu + ig'Y_R B_\mu) \psi_R$
    - $g$  and  $g'$  are boson coupling constants. <sup>1</sup>
    - $W_\mu = \sigma^i W_\mu^i$ , where  $\sigma^i$  are the pauli matrices.

<sup>1</sup>L(R) refers to Left and right fields. Y is the weak hypercharge,  $Y = T^3 - Q$ . Q is charge of particle field and T is weak isospin.  $T^3 = \pm 1/2$  for left handed doublets and  $T^3 = 0$  for right handed singlets. ▶◀☰☰☰☰☰☰☰ 7/79



## Electroweak SM Lagrangian

## Higgs lagrangian

$$\mathcal{L}_{\text{Higgs}} = (D_\mu \Phi)^\dagger (D^\mu \Phi) - V(\Phi^\dagger \Phi) \quad (1)$$

with

- $D_\mu \Phi = \left( \partial_\mu + (ig/2)\sigma^i W_\mu^i - i\frac{1}{2}g' B_\mu \right) \Phi$
  - $V(\Phi^\dagger \Phi) = -\mu^2 \Phi^\dagger \Phi + \frac{1}{2}\lambda(\Phi^\dagger \Phi)^2, \quad \mu^2 > 0$
  - $\Phi = \begin{pmatrix} \phi^+ \\ \phi^0 \end{pmatrix}$  is a SU(2) doublet.
  - $\sigma^i$  are the Pauli matrices.
  - $\Phi$  is higgs field which is a complex scalar field.  $\Phi$
  - $\lambda$  and  $\mu^2$  are Higgs potential parameters



# SM Lagrangian

## Yukawa lagrangian

$$\mathcal{L}_{yukawa} = \Gamma_{mn}^u q_{m,L} \tilde{\phi} u_{n,R} + \Gamma_{mn}^d \bar{q}_{m,L} \phi d_{n,R} + \Gamma_{mn}^e \bar{l}_{m,L} \phi e_{n,R} + h.c \quad (2)$$

where h.c is hermitian conjugate.

The matrices  $\Gamma_{mn}$  describe the so called Yukawa couplings between higgs doublet  $\phi$  and the fermions.

Choosing

$$\Phi = -\frac{1}{2} \begin{pmatrix} 0 \\ v + h \end{pmatrix} \rightarrow \Phi = \frac{1}{2} \begin{pmatrix} 0 \\ v \end{pmatrix}$$

By using it on the first part of the lagrangian it is obtained for u quark

$$\mathcal{L}_{yukawa} = \frac{\Gamma_{uu}^u v}{\sqrt{2}} (\bar{u}_L u_R + \bar{u}_R u_L)$$

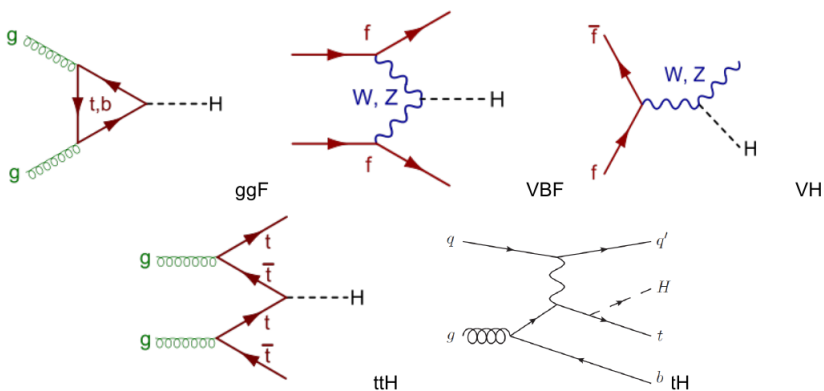
from which the masses for the fermions in question can be read off:

$$m_u = -\frac{\Gamma_{uu}^u v}{\sqrt{2}}$$

which m is the mass of fermions.



# Higgs production mechanisms



Different Higgs production mechanism, from the most likely to least likely

# tH production mechanisms

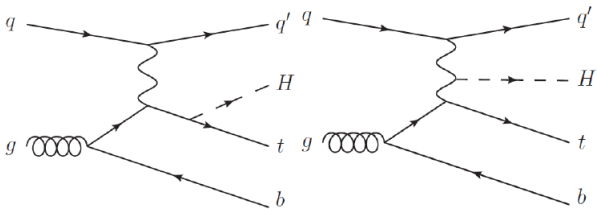


**Figure:** tH mechanism. Higgs radiated from a top quark (left). Higgs radiated from a W boson (right)

## tH production mechanisms

- In a proton proton collision, the production cross section of the single top plus Higgs boson ( $tHq$ ) process is driven by a destructive interference of two main diagrams (see Fig. 1.), where the Higgs couples to either the  $W$  boson or the top quark.
  - A second process, where the Higgs and top quark are accompanied by a  $W$  boson ( $tHW$ ) has similar behavior, albeit with a weaker interference pattern.
  - However, in the presence of new physics, there may be relative opposite signs between the  $tH$  and  $WH$  couplings which lead to constructive interference and enhance the cross sections by an order of magnitude or more.

# Cross section

- Classical definition: When two particles interact, cross section is the area transverse to their relative motion within which they must meet in order to scatter from each other.
- Quantum definition: Cross section describes the likelihood of two particles interacting under certain conditions[1][8]
- Experimentally

$$d\sigma = \frac{\text{number of particles scattered into solid angle } \Delta\Omega}{(\text{number of particles incident})(\text{scattering centers/area})} \quad (3)$$

- Cross sections are expressed in barns , where  $1 \text{ barn} = 10^{-34} \text{ cm}^{-2}$

# Cross section

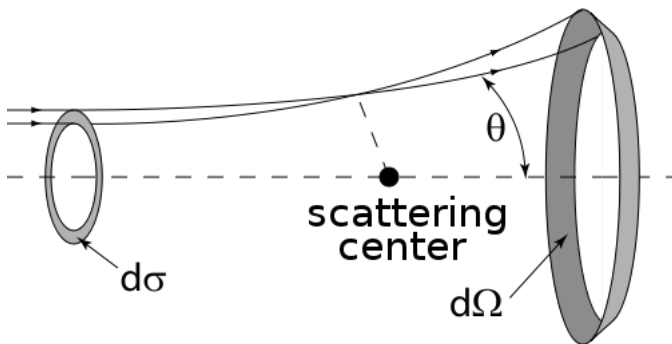


Figure: Drawing of an idealized scattering process showing the differential solid angle  $\Delta\Omega$  and the scattering angle  $\theta$

# Cross section

The reaction rate  $N_R$  is determined by the total cross section  $\sigma$  and the incident flux  $L$ .

$L$  is called luminosity and it is measured in  $\text{cm}^{-1}\text{s}^{-1}$ .[8]

$$N_R = \sigma L \quad (4)$$

# Higgs production Cross section

Higgs boson production cross sections in pp collisions for  $\sqrt{s} = 13\text{TeV}$  (in pico barn). Integrated luminosity of  $35.9\text{ fb}^{-1}$  for Run 2<sup>2</sup>

Production mechanism	$\sigma$ (picobarns pb)	Number of events
ggF	48.93	1756587
VBF	3.78	135702
WH	1.35	48465
ZH	0.88	31592
t $\bar{t}$ H	0.50	18255
tH (only)	0.015	560.39

<sup>1</sup>Data taken from The cern collaborarion "Higgs Physics the HL-LHC and HE-LHC" 2019,  
CERN-LPCC-2018-04

# Higgs production cross section

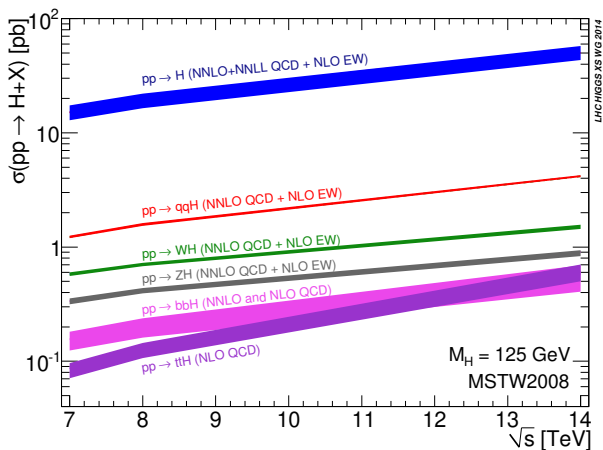


Figure: Higgs boson production cross sections as a function of the centre-of-mass-energies

# Branching ratio

In particle physics, the branching ratio for a decay process is the ratio of the number of particles which decay via a specific decay mode with respect to the total number of particles which decay via all decay modes.

3

$$\text{BR} = \frac{\Gamma_i}{\sum_i \Gamma_i} \quad (5)$$

Where  $\Gamma = \sum_i \Gamma_i$  is the total decay width (sum of all partial widths) of the particle and is related to lifetime of the particle:  $\Gamma = 1/\tau$ . Since the dimension of  $\Gamma$  is the inverse of time, in our system of natural units, it is measured in inverse seconds.<sup>0</sup>

<sup>0</sup> Cleaves H.J. (2011) Branching Ratio. In: Gargaud M. et al. (eds) Encyclopedia of Astrobiology. Springer, Berlin, Heidelberg

# Higgs Branching ratio

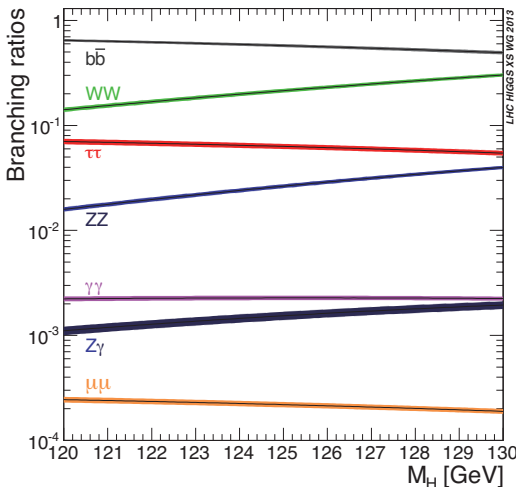


Figure: Standard Model Higgs boson decay branching ratios

# Higgs Branching ratios per channel

SM Higgs boson branching ratios for  $M_H = 125$  GeV

Higgs decay	Branching ratio (BR)
$H \rightarrow b\bar{b}$	50.82%
$H \rightarrow W^+W^-$	21.5%
$H \rightarrow \tau^+\tau^-$	6.27%
$H \rightarrow ZZ$	2.61%
$H \rightarrow \gamma\gamma$	0.227%
$H \rightarrow Z\gamma$	0.153%
$H \rightarrow \mu^+\mu^-$	0.0217%

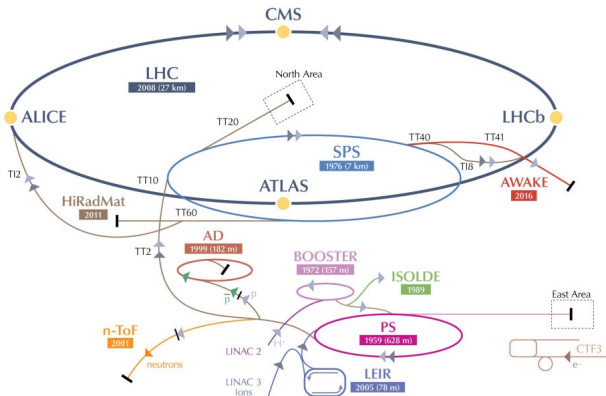
# $\mu\mu$ same sign decay rate

Table of decay chains for tH. Expected number of final events assuming 560 produced tH events. l represents  $\mu^\pm, e^-, \tau^\pm$ .

Decay chain	BR	Events
$tH \rightarrow W^+ b W^+ W^- \rightarrow \mu^+ \nu_\mu b \mu^+ \nu_\mu q \bar{q}'$	$2.096 \times 10^{-3}$	1.173
$tH \rightarrow W^+ b W^+ W^- \rightarrow \mu^+ \nu_\mu b \mu^+ \nu_\mu l^- \bar{\nu}_l$	$3.37 \times 10^{-4}$	0.899
$tH \rightarrow W^+ b \tau^+ \tau^- \rightarrow \mu^+ \nu_\mu b \mu^+ \nu_\mu \bar{\nu}_\tau l^- \bar{\nu}_l \nu_\tau$	$3.637 \times 10^{-4}$	0.203
$tH \rightarrow W^+ b W^+ W^- \rightarrow \tau^+ \bar{\nu}_\tau b \mu^+ \nu_\mu q \bar{q} \rightarrow \mu^+ \nu_\mu \bar{\nu}_\tau \bar{\nu}_\tau b \mu^+ \nu_\mu q \bar{q}$	$1.890 \times 10^{-4}$	0.105
$tH \rightarrow W^+ b \tau^+ \tau^- \rightarrow \mu^+ \nu_\mu b \nu_\tau \mu^+ \nu_\mu \bar{\nu}_\tau q \bar{q}$	$1.681 \times 10^{-4}$	0.094
$tH \rightarrow W^+ b W^+ W^- \rightarrow \tau^+ \bar{\nu}_\tau b \mu^+ \nu_\mu l^- \bar{\nu}_l \rightarrow \mu^+ \nu_\mu \bar{\nu}_\tau \bar{\nu}_\tau b \mu^+ \nu_\mu l^- \bar{\nu}_l$	$3.045 \times 10^{-5}$	0.017
$tH \rightarrow W^+ b ZZ \rightarrow q \bar{q} b ZZ \rightarrow q \bar{q} b \mu^+ \mu^- \mu^+ \mu^-$	$1.966 \times 10^{-5}$	0.011
$tH \rightarrow W^+ b \tau^+ \tau^- \rightarrow \tau^+ \bar{\nu}_\tau b \mu^+ \nu_\mu \bar{\nu}_\tau q \bar{q}' \nu_\tau \rightarrow \mu^+ \nu_\mu \bar{\nu}_\tau \bar{\nu}_\tau b \mu^+ \nu_\mu \bar{\nu}_\tau q \bar{q}' \nu_\tau$	$1.549 \times 10^{-5}$	0.008

## LHC

## CERN's Accelerator Complex



## LHC parameters

Quantity	Number
Circumference	26 659 m
Dipole operating temperature	1.9 K (-271.3°C)
Number of magnets	9593
Number of main dipoles	1232
Number of main quadrupoles	392
Number of RF cavities	8 per beam
Nominal energy, protons	6.5 TeV
Nominal energy, ions	2.56 TeV/u (energy per nucleon)
Nominal energy, protons collisions	13 TeV
No. of bunches per proton beam	2808
No. of protons per bunch (at start)	$1.2 \times 10^{11}$
Number of turns per second	11245
Number of collisions per second	1 billion

Table. LHC characteristics for run 2.

# LHC

## Accelerator operation energies

Accelerator	Energy
Linac 2	50 MeV
PS Booster	1.4 GeV
Proton Scyncroton (PS)	25 GeV
SPS	450 GeV
LHC	6.5 TeV

# CMS detector

## CMS DETECTOR

Total weight : 14,000 tonnes  
Overall diameter : 15.0 m  
Overall length : 28.7 m  
Magnetic field : 3.8 T

STEEL RETURN YOKE  
12,500 tonnes

SILICON TRACKERS  
Pixel (100x150  $\mu$ m)  $\sim 16m^2$   $\sim 66M$  channels  
Microstrips (80x180  $\mu$ m)  $\sim 200m^2$   $\sim 9.6M$  channels

SUPERCONDUCTING SOLENOID  
Niobium titanium coil carrying  $\sim 18,000A$

MUON CHAMBERS  
Barrel: 250 Drift Tube, 480 Resistive Plate Chambers  
Endcaps: 468 Cathode Strip, 432 Resistive Plate Chambers

PRESHOWER  
Silicon strips  $\sim 16m^2$   $\sim 137,000$  channels

FORWARD CALORIMETER  
Steel + Quartz fibres  $\sim 2,000$  Channels

CRYSTAL  
ELECTROMAGNETIC  
CALORIMETER (ECAL)  
 $\sim 76,000$  scintillating PbWO<sub>4</sub> crystals

HADRON CALORIMETER (HCAL)  
Brass + Plastic scintillators  $\sim 7,000$  channels

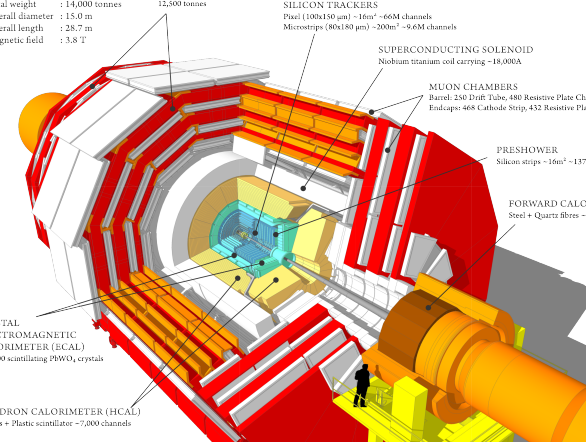


Figure: Compact muon solenoid

CMS integrated luminosity

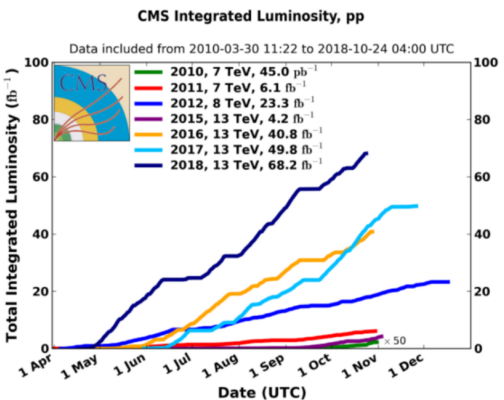
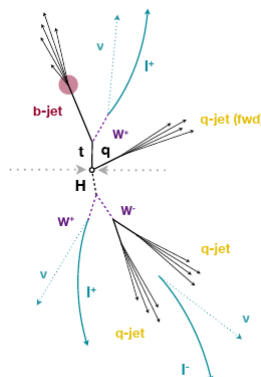


Figure: Integrated luminosity for CMS experiment

## Topology of events tH

### The characteristics of the signal th:

- $t \rightarrow W^+ b \rightarrow l^+ \nu_\mu b$
  - $H \rightarrow W^+ W^-$ 
    - $W \rightarrow l^\pm \nu$ , where  $l$  can be  $\mu^\pm, e^\pm, \tau^\pm$
    - $W \rightarrow q\bar{q}$
    - $W$  bosons decay leptonically resulting in a signature of two same-sign leptons
  - a light-flavor quark
  - b quark jet [2]



# Event selection

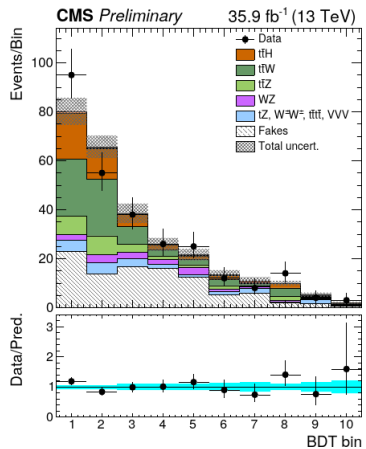
The main analysis strategy is to obtain a selection of events compatible with certain characteristics of the signal at pre-selection level.

It is required:

- The events are selected those that contain two leptons ( $l^+l^-$ ) with the same sign.
- Transverse moment  $p_t > 25$  and  $15$  GeV, for the muons.
- A foward jet with  $p_t > 40$  GeV,  $| \eta | > 2.4$
- One or more b-jets with ( $| \eta | < 2.4$ )[1]

## Previous results for $t\bar{t}H + tH$ production

Process	$\mu_F$
$t\bar{t}W^\pm$	$68.03 \pm 0.61$
$t\bar{t}Z/t\bar{t}\gamma$	$25.89 \pm 1.12$
$WZ$	$15.07 \pm 1.19$
$ZZ$	$1.16 \pm 0.29$
$W^\pm W^\pm qq$	$3.96 \pm 0.52$
$W^\pm W^\pm (\text{DPS})$	$2.48 \pm 0.42$
$VVV$	$2.99 \pm 0.34$
$ttt\bar{t}$	$2.32 \pm 0.45$
$tZq$	$5.77 \pm 2.24$
$tZW$	$2.13 \pm 0.13$
$\gamma$ conversions	—
Non-prompt	$80.94 \pm 2.02$
Charge flips	—
Total Background	$210.74 \pm 3.61$
$t\bar{t}H$	$24.18 \pm 0.48$
$tHq$ (SM)	$1.43 \pm 0.04$
$tHW$ (SM)	$0.71 \pm 0.03$
Total SM	$237.06 \pm 3.64$
$tHq$ ( $\kappa_V = 1 = -\kappa_t$ )	$18.48 \pm 0.22$
$tHW$ ( $\kappa_V = 1 = -\kappa_t$ )	$7.72 \pm 0.17$
Data	280



Post-fit categorized BDT classifier outputs as used in the maximum likelihood fit for the  $\mu\mu$  channel for 35.9  $\text{fb}^{-1}$ . In the box below each distribution, the ratio of the observed and predicted event yields is shown. [2]

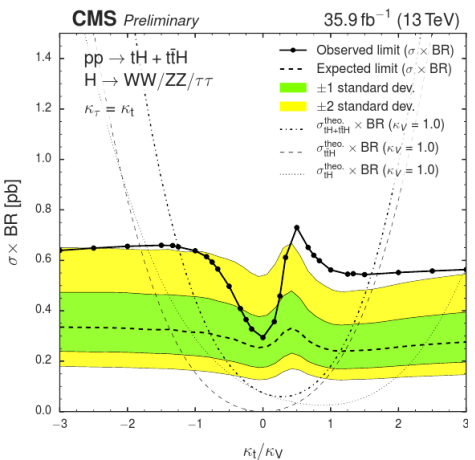


**Figure:** Observed and expected 95% C.L. upper limit on the  $tH + t\bar{t}H$  cross section times  $H \rightarrow WW + \tau\tau + ZZ$  branching fraction for different 20 values of the coupling ratio  $\kappa_t/\kappa_V$ . The expected limit is derived from a background-only MC dataset.

# Main backgrounds

Background	$\sigma[\text{pb}]$	Decay process
t $\bar{t}$ H	0.2151	$t\bar{t}H \rightarrow W^+b W^- \bar{b} W^+W^- \rightarrow \mu^+\nu_\mu b \mu^-\bar{\nu}_\mu \bar{b} \mu^+\nu_\mu \mu^-\bar{\nu}_\mu$
t $\bar{t}$ W	0.2043	$t\bar{t}W \rightarrow W^+b W^- \bar{b} \mu^+\nu_\mu \rightarrow \mu^+\nu_\mu b \mu^-\bar{\nu}_\mu \bar{b} \mu^+\nu_\mu$
t $\bar{t}$ Z	0.2529	$t\bar{t}Z \rightarrow W^+b W^- \bar{b} \mu^+\mu^- \rightarrow \mu^+\nu_\mu b \mu^-\bar{\nu}_\mu \bar{b} \mu^+\mu^-$
W $^\pm$ W $^\pm$	1.64	$W^+W^- \rightarrow \mu^+\nu_\mu \mu^-\bar{\nu}_\mu$
tZq	0.0758	$tZq \rightarrow W^+b \mu^+\mu^- q \rightarrow \mu^+\nu_\mu b \mu^-\bar{\nu}_\mu \bar{b} \mu^+\mu^- q$
t $\bar{t}t\bar{t}$	0.0091	$t\bar{t}t\bar{t} \rightarrow W^+b W^- \bar{b} W^+b W^- \bar{b} \rightarrow \mu^+\nu_\mu b \mu^-\bar{\nu}_\mu \bar{b} \mu^+\nu_\mu b \mu^-\bar{\nu}_\mu \bar{b}$
W $^+W^-Z$	0.1651	$W^+W^-Z \rightarrow \mu^+\nu_\mu \mu^-\bar{\nu}_\mu \mu^+\mu^-$
ZZZ	0.0139	$ZZZ \rightarrow \mu^+\mu^-\mu^+\mu^- l^+l^-$
W $^+ZZ$	0.0556	$W^+ZZ \rightarrow \mu^+\nu_\mu \mu^+\mu^- l^+l^-$
W $^+Z$	4.42965	$W^+Z \rightarrow \mu^+\nu_\mu \mu^+\mu^-$
ZZ	1.256	$ZZ \rightarrow \mu^+\mu^-\mu^+\mu^-$

- Rare SM: tt $\bar{t}$ t $\bar{t}$ ,WW $^\pm$ ,WWZ,WZZ,WW,tZq
- WZ:WZ,ZZ

# Boosted decision tree (BDT)

- A decision tree takes a set of input features and splits input data recursively based on those features. Boosting is a method of combining many weak learners (trees) into a strong classifier. The features can be a mix of categorical and continuous data.
- The BDT training is performed using several event variables for signal and background.
- BDT training uses MC samples for  $t\bar{t}W^\pm$  and  $t\bar{t}Z$  ( $t\bar{t}V$ ), because  $t\bar{t}V$  is one of the biggest backgrounds

# BDT Variables

- Trailing lepton  $p_t$
- Total charge of tight leptons
- $\min \Delta R$  (lepton pairs)
- $\Delta\phi$  between highest  $p_t$  lepton pair
- Number of jets with  $|\eta| < 2.4$
- Number of non b-tagged jets with  $|\eta| > 1.0$
- Maximum  $|\eta|$  for jets
- $\Delta\eta$  (most forward light jet, closest lepton)
- $\Delta\eta$  (most forward light jet, hardest loosely b-tagged jet)
- $\Delta\eta$  (most forward light jet, 2nd hardest loosely b-tagged jet)

# Sources of uncertainty on event yields

- Luminosity measurement: 2.6%.
- Data/MC scale factors for lepton selection (ID, iso) and trigger efficiencies 5% per lepton.
- Choice of PDF set:
  - 3.7% for tHq
  - 4% for tHW,  $t\bar{t}W$ ,  $t\bar{t}Z$ ,  $t\bar{t}H$
  - Scale uncertainties: 12%, 4% for  $t\bar{t}W$ , 10% for  $t\bar{t}Z$ , +5.8/-9.2% for  $t\bar{t}H$ .
- Background: WZ, ZZ sample modelling and statistics: 50%.
- Rare SM (tZ, tri-bosons, WWqq, tt) : 50%
- Fake rate estimation: The predicted event yield has a normalization uncertainty of 30-50% [7]

## Uncertainty values

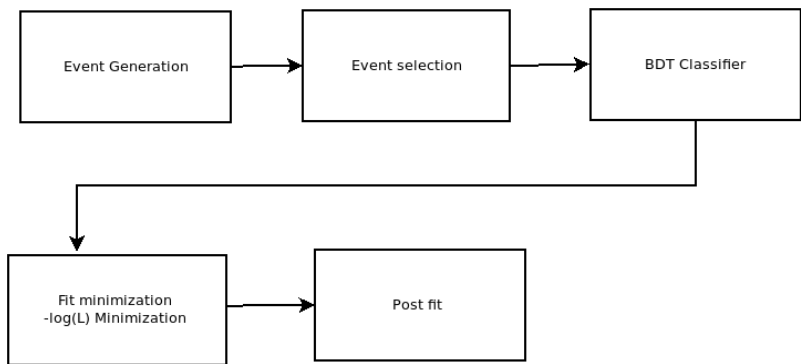
### Common uncertainties for MC :

- Muon identificacion 6%
  - Dimuon Trigger 1%

Background	Sources of systematic uncertainty	Total Systematic Uncertainty
$t\bar{t}H$	<ul style="list-style-type: none"> <li>PDF 4%</li> <li>QCD scale 5.8%</li> <li>Higgs BR 1%</li> </ul>	9.36%
$t\bar{t}Z$	<ul style="list-style-type: none"> <li>PDF 4%</li> <li>QCD scale 10%</li> </ul>	12.36 %
$t\bar{t}W$	<ul style="list-style-type: none"> <li>PDF 4%</li> <li>QCD scale 12%</li> </ul>	14.03 %

Background	Sources of systematic uncertainty	Total Systematic Uncertainty
Rares SM	<ul style="list-style-type: none"> <li>• Rare SM 50%</li> </ul>	50.36 %
WZ	<ul style="list-style-type: none"> <li>• Sample modelling and statistics 50%</li> </ul>	50.36%
Non prompt leptons	<ul style="list-style-type: none"> <li>• Fake rate estimation 50%</li> <li>• Closure 7%</li> </ul>	50.48%

# Fitting



# Likelihood model

The likelihood function is the product of Poisson probabilities for all bins

$$L(\mu, \theta) = \prod_{j=1}^N \frac{(\mu s_j + b_j)^{n_j}}{n_j!} e^{-(\mu s_j + b_j)} \quad (6)$$

- N=number of bins
- $\mu$ =parameter of signal
- $s$ =signal
- $b$ =background
- $n$ =number of events

# Results

## Likelihood scan

To test a hypothesized value of  $\mu$  we consider the profile likelihood ratio

$$\lambda(\mu) = \frac{L(\mu, \hat{\theta})}{L(\hat{\mu}, \hat{\theta})} \quad (7)$$

- Here  $\hat{\theta}$  in the numerator denotes the value of  $\theta$  that maximizes  $L$  for the specified  $\mu$ , it is the conditional maximum-likelihood (ML) estimator of  $\hat{\theta}$  (and thus is a function of  $\mu$ ). The denominator is the maximized (unconditional) likelihood function, i.e.,  $\hat{\mu}$  and  $\hat{\theta}$  are their ML estimators[4].
- The presence of the nuisance parameters broadens the profile likelihood as a function of  $\mu$  relative to what one would have if their values were fixed. This reflects the loss of information about  $\mu$  due to the systematic uncertainties[4][6].

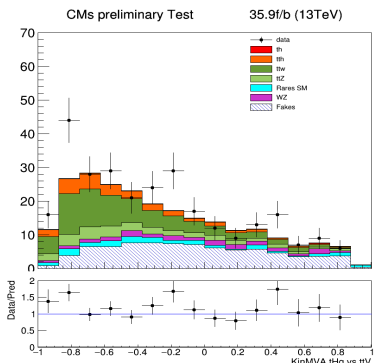
# Statistical test

It is convenient to use the statistic

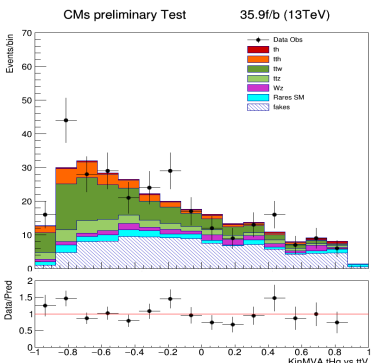
$$t_\mu = -2 \ln \lambda(\mu) \quad (8)$$

as the basis of a statistical test. Higher values of  $t_\mu$  thus correspond to increasing incompatibility between the data and  $\mu$ . We may define a test of a hypothesized value of  $\mu$  by using the statistic  $t_\mu$  directly as measure of discrepancy between the data and the hypothesis, with higher values of  $t_\mu$  correspond to increasing disagreement[6]

## Results



Pre-fit signal and background yields for tH process. In the box below each distribution, the ratio of the observed and predicted event yields is shown



Post-fit signal and background yields for tH process. In the box below each distribution, the ratio of the observed and predicted event yields is shown

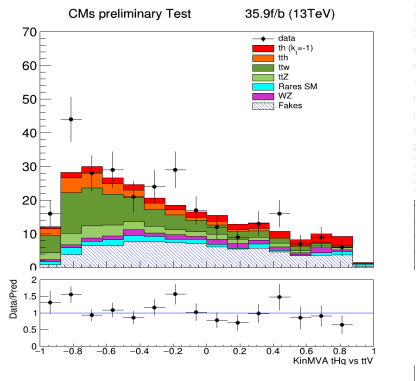
## Results

Table: Prefit and postfit table for each yield.

Process	Number of events prefit	Number of events Postfit
tH	2.13	$5.36 \pm 27.40$
t <bar>t&gt;H</bar>	$24.18 \pm 2.26$	$24.81 \pm 2.24$
t <bar>t&gt;W</bar>	$68.03 \pm 9.54$	$77.01 \pm 8.76$
t <bar>t&gt;Z</bar>	$25.89 \pm 3.20$	$26.74 \pm 3.18$
Rares SM	$17.17 \pm 8.64$	$18.77 \pm 8.66$
WZ	$16.23 \pm 8.17$	$17.41 \pm 8.04$
fakes	$80.94 \pm 40.86$	$100.15 \pm 29.30$

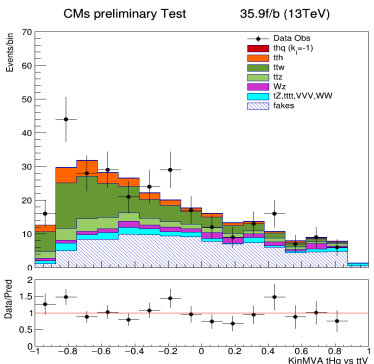
Prefit uncertainty is statistical only. Postfit uncertainty is statistical + systematic.

## Results



Pre-fit signal and background yields for tH process for  $k_t = -1$ .

In the box below each distribution, the ratio of the observed and predicted event yields is shown



Post-fit signal and background yields for tH process for  $k_t = -1$ .

In the box below each distribution, the ratio of the observed and predicted event yields is shown

## Results

Table: Prefit and postfit table for each yield.  $k_t = -1$ .

Process	Number of events prefit	Number of events Postfit
tH	26.2	$1.83 \pm 26.63$
t <bar>t}H</bar>	$24.18 \pm 2.26$	$24.82 \pm 2.27$
t <bar>t}W</bar>	$68.03 \pm 9.54$	$77.07 \pm 8.99$
t <bar>t}Z</bar>	$25.89 \pm 3.20$	$26.76 \pm 3.18$
Rares SM	$17.17 \pm 8.64$	$18.90 \pm 8.37$
WZ	$16.23 \pm 8.17$	$17.54 \pm 8.15$
fakes	$80.94 \pm 40.86$	$102.97 \pm 29.51$

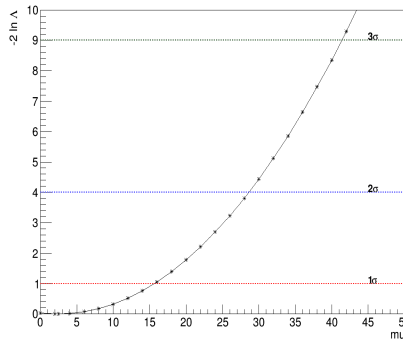
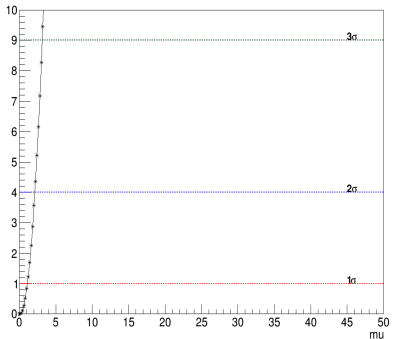
Prefit uncertainty is statistical only. Postfit uncertainty is statistical + systematic.

## Test statistic $q_\mu$ for upper limits

For purposes of establishing an upper limit on the strength parameter  $\mu$ , we consider two closely related test statistics. First, we may define

$$q_\mu = \begin{cases} -2 \ln \lambda(\mu) & \hat{\mu} \leq \mu \\ 0 & \hat{\mu} < 0 \end{cases}$$

The reason for setting  $q_\mu = 0$  for  $\hat{\mu} > \mu$  is that when setting an upper limit, one would not regard data with  $\hat{\mu} > \mu$  as representing less compatibility with  $\mu$  than the data obtained, and therefore this is not taken as part of the rejection region of the test. From the definition of the test statistic one sees that higher values of  $q_\mu$  represent greater incompatibility between the data and the hypothesized value of  $\mu$ .

Likelihood scan for  $k_t=1$  (SM)Likelihood scan for  $k_t=-1$

# Test statistic $q_\mu$ for upper limits

Table for estimation of  $\mu$  for fitting and upper limit with luminosity of  $35.9 \text{ fb}^{-1}$  with 95% of confidence

Model	$\mu$	$\mu$ upper limit
SM ( $k_t = 1$ )	$2.497 \pm 12.9$	28.047
$k_t = -1$	$0.0693 \pm 1.02$	1.97

# P value

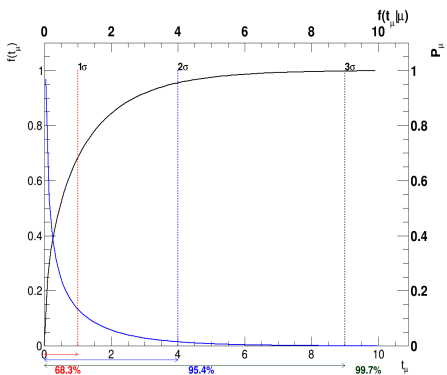
To quantify the level of disagreement we compute the P-value

$$P_\mu = \int_{t_\mu}^{\infty} f(t_\mu|\mu) dt_\mu \quad (9)$$

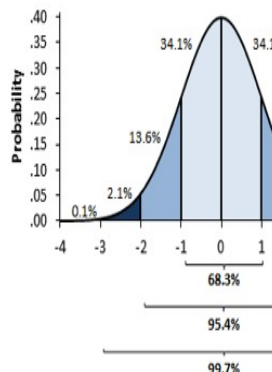
where  $t_\mu$  is the value of the statistic  $t_\mu$  observed from the data and  $f(t_\mu|\mu)$  denotes the PDF (Probability density function) of  $t_\mu$  under the assumption of the signal strength  $\mu$  [6]

$$f(t_\mu|\mu) = \frac{1}{\sqrt{2\pi}} \frac{1}{\sqrt{t_\mu}} e^{\frac{-t_\mu}{2}} \quad (10)$$

# P Value and significance

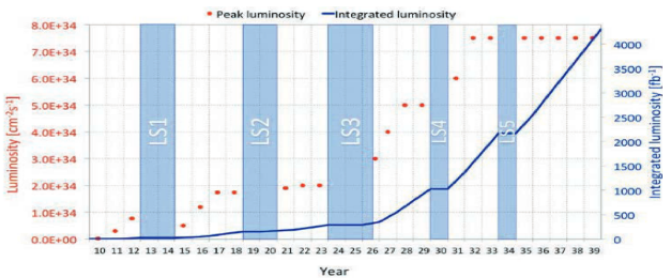


P value and significance for  $t_\mu$



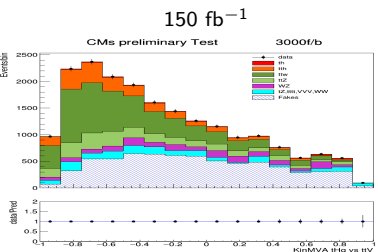
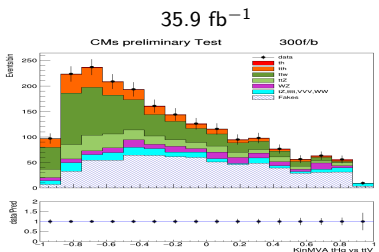
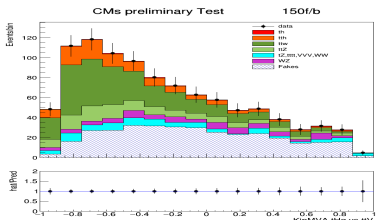
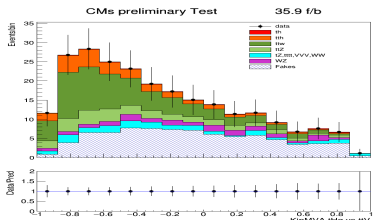
A Gaussian distribution with sig

# Luminosity

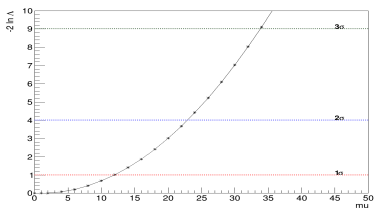


Graph of luminosity of LHC measured and expected through years[8]

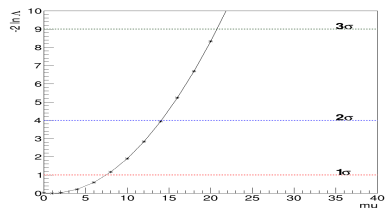
## Extrapolation of luminosity for SM



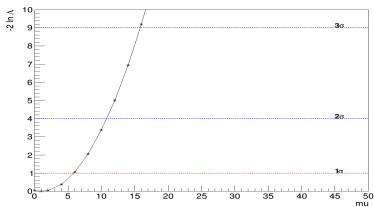
## Likelihood scan for SM



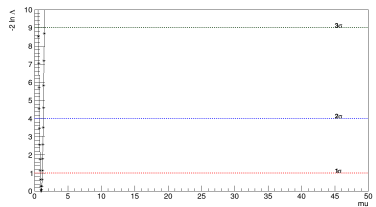
35.9 fb<sup>-1</sup>



150 fb<sup>-1</sup>

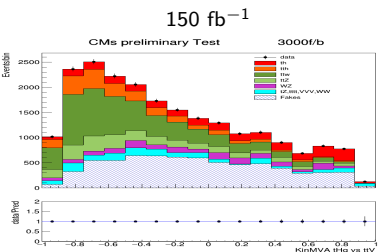
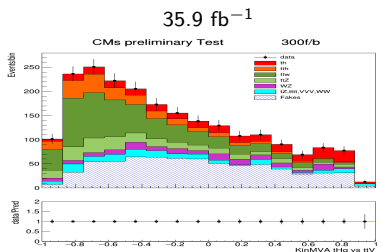
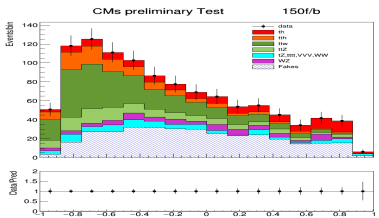
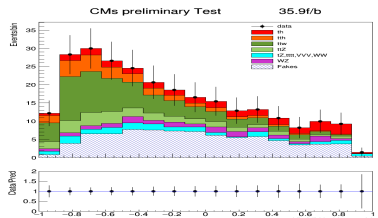


300 fb<sup>-1</sup>

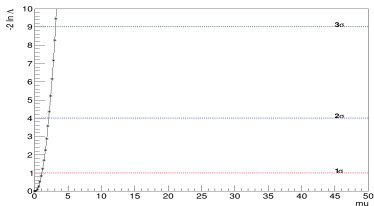


3000 fb<sup>-1</sup>

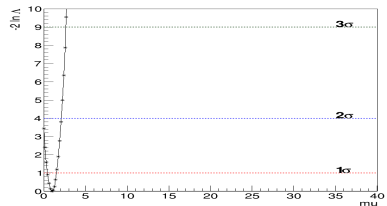
### Extrapolation of luminosity for $k_t = -1$



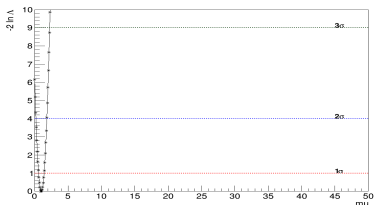
### Likelihood scan for $k_t = -1$



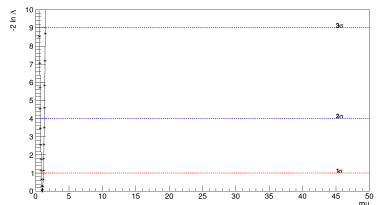
35.9 fb<sup>-1</sup>



150 fb<sup>-1</sup>



300 fb<sup>-1</sup>



3000 fb<sup>-1</sup>

## Results

## Estimation of $\mu$ and upper limits for extrapolations

Luminosity (fb $^{-1}$ )	$\mu$	$\mu$ for $k_t = -1$	$\mu$ upper limit	$\mu$ upper limit for $k_t = -1$
35.9	$1.00 \pm 8.32$	$1.00 \pm 0.249$	22.328	2.777
150	$1.00 \pm 6.44$	$1.00 \pm 0.544$	12.619	0.915
300	$1.00 \pm 4.83$	$1.00 \pm 0.407$	9.427	0.649
3000	$1.00 \pm 1.54$	$1.00 \pm 0.151$	3.442	0.25

# Conclusions

- We analyzed the tH process produced from PP collisions for the production of  $\mu\mu$  final states
- We discussed about events selections for the 2016 and by using BDT process, separate signal and background data.
- The creation of a model with systematic uncertainties to make a minimization (fit) and obtain a fit which is compatible with Standard Model.
- two models are included for comparison
- Generation of likelihood scan for the exclusion of data and obtain the probability of detection of a Higgs boson.
- Generating simulations for predict results with higher luminosities, according to the future experiments.

# References

-  Gross F. *Relativistic quantum mechanics and field theory*, 1994, WILEY-VCH Verlag GmbH & Co. KGaA
-  Griffiths, D. *Introduction to Elementary Particles*, 2<sup>nd</sup> edition, 2008, WILEY-VCH Verlag GmbH & Co. KGaA
-  The CMS collaboration, *Search for production of a Higgs boson and a single top quark in multilepton final states in proton collisions at 13 TeV*, CMS-PAS-HIG-17-005 .arXiv:1811.09696
-  Verkerke W *Dealing with systematic uncertainties* 2014. From [https://indico.cern.ch/event/287744/contributions/1641261/attachments/535763/738679/Verkerke\\_Statistics\\_3.pdf](https://indico.cern.ch/event/287744/contributions/1641261/attachments/535763/738679/Verkerke_Statistics_3.pdf)

-  ATLAS and CMS Collaborations, *Combined measurement of the Higgs boson mass in  $pp$  collisions at  $\sqrt{s} = 7$  and  $8$  TeV with the ATLAS and CMS experiments*, Phys. Rev. Lett. 114 (2015) doi:10.1103/PhysRevLett.114.191803, arXiv:1503.07589
-  Cowan G. , Cranmer K., Gross E. , Vitells O. *Asymptotic formulae for likelihood-based tests of new physics* 2013 , arXiv:1007.1727
-  CMS collaboration *Search for  $tHq$  production in multilepton final states at 13 TeV* ,2017,CMS AN-16-378
-  CMS collaboration *High-Luminosity Large Hadron Collider (HL-LHC)*, 2017,CERN-2017-007-M

# Back up

# Main backgrounds

In the leptonic channels, the main backgrounds are expected to arise from the production of top quarks

- In the dominant  $t\bar{t}$  mode, where same-sign dilepton signatures can occur when a non-prompt lepton from heavy-flavor decay passes the signal selection, or in associated production with a W/Z or Higgs boson.
- Processes with single top quarks also contribute, mostly in the associated production with a Z boson (tZ) or when produced with both a W and a Z boson (WZ)

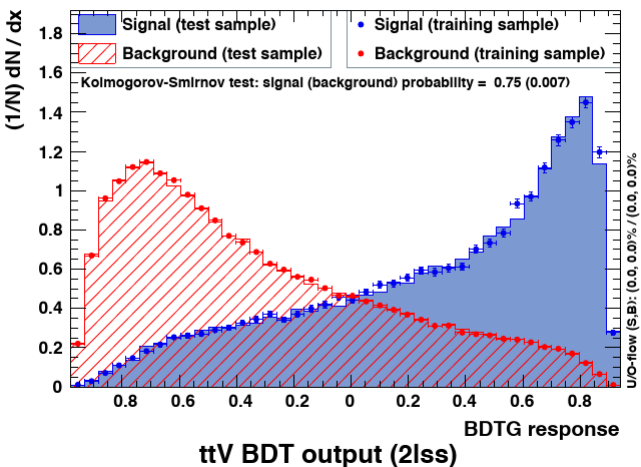
# Main backgrounds

- $t\bar{t}W^\pm$  and  $t\bar{t}Z$  ( $t\bar{t}V$ ): Backgrounds are estimated directly from simulated events
- WZ: Diboson production with leptonic Z decays and additional jet radiation in the final state can lead to signatures very similar to that of the signal. Due to the larger cross section, the main contribution arises from WZ production.
- $t\bar{t}H$ : tHq production which decays to same sign dileptons.
- Rare SM ( $tZ, VVV, WW, tttt$ ): Due to small event yields, all these processes are grouped as one.
- Non prompt leptons b quark decays and spurious lepton signatures from hadronic jets.

# BDT parameters

- Gradient boosted (BDTG)
- No. of trees = 800
- No. of cuts = 50
- Maximum depth = 3
- Found to be most discriminating, minimal overtraining.

TMVA overtraining check for classifier: BDTG



## List of histograms used in the analysis

Data taken from the file plots-thq-2lss-kinMVA.root 2016  
CERN

thqMVA\_ttv\_2lss\_40\_tZq  
thqMVA\_ttv\_2lss\_40\_ttZ  
thqMVA\_ttv\_2lss\_40\_VVV  
thqMVA\_ttv\_2lss\_40\_ttW  
thqMVA\_ttv\_2lss\_40\_data\_fakes  
thqMVA\_ttv\_2lss\_40\_ttH  
thqMVA\_ttv\_2lss\_40\_thW\_hww  
thqMVA\_ttv\_2lss\_40\_WWss  
thqMVA\_ttv\_2lss\_40\_tttt  
thqMVA\_ttv\_2lss\_40\_WZ  
thqMVA\_ttv\_2lss\_40\_thQ\_hww

## Backgrounds and signal histograms

### tHq: Signal (tH)

- thqMVA\_ttv\_2lss\_40\_tHq\_hww
  - thqMVA\_ttv\_2lss\_40\_tHW\_hww

## Backgrounds

t $\bar{t}$ W

- thqMVA\_ttv\_2lss\_40\_ttW

t $\bar{t}$ Z

- thqMVA\_ttv\_2lss\_40\_ttZ

wz

- thqMVA\_ttv\_2lss\_40\_WZ

## Backgrounds and signal histograms

## Backgrounds

tZ, VVV, tttt, WW;

- thqMVA\_ttv\_2lss\_40\_tZq
  - thqMVA\_ttv\_2lss\_40\_WWss
  - thqMVA\_ttv\_2lss\_40\_VVV
  - thqMVA\_ttv\_2lss\_40\_tttt

t<sup>−</sup>tH

- thqMVA\_ttv\_2lss\_40\_ttH

### Non prompt leptons (fakes)

- thqMVA\_ttv\_2lss\_40\_data\_fakes

Closure: hay jets en los eventos de  $t\bar{t}$  (gluon-gluon  $\rightarrow t\bar{t} + \text{gluon}$ ) que se pasan como muones. jet  $\rightarrow$  muon = fake

Fakes: proceso de QCD que genera muchos jets (por ejemplo gluon-gluon  $\rightarrow$  gluons, quarks) : jet  $\rightarrow$  muons fakes are estimated data

1

---

<sup>1</sup>Due to existence of many uncertainties, it is necessary to sum all the uncertainties. When there is no Correlation, the uncertainties must be summed as the square root of the squares of each uncertainty

# Sources of systematic uncertainty

## Detector-simulation related uncertainty

- Calibrations (electron, jet energy scale)
- Efficiencies (particle ID, reconstruction)
- Resolutions (jet energy, muon momentum)

## Theoretical uncertainties

- Factorization/Normalization scale of MC generators
- Choice of MC generator (ME and/or PS, e.g. Herwig vs Pythia)

## Monte Carlo Statistical uncertainties

- Statistical uncertainty of simulated samples[2]

# Observed events

- After applying the event pre-selection on the dataset, 280 events are observed in the same-sign  $\mu\mu$  channel
- The events are then sorted into ten categories depending on the output of the two BDT classifiers according to an optimized binning strategy, resulting in a one-dimensional histogram with ten bins.
- In each point, the tH and  $t\bar{t}H$  production cross sections and the Higgs decay branching ratios are modified with the Higgs-top ( $\kappa_t$ ) and Higgs-vector boson ( $\kappa_v$ ) coupling strength.
- The Higgs-tau coupling strength modifier ( $\kappa_\tau$ ) is assumed to be equal to  $\kappa_t$ .
- All other parameters are assumed to be at the values predicted by the standard model[1].

### $\alpha$ values for post fit

Floating Parameter	FinalValue	+/- Error
Lumi	1.0082e+00	+/- 2.42e-02
alpha_sample_tth_sys	1.9100e-01	+/- 9.94e-01
alpha_sample_ttw_sys	8.7537e-01	+/- 9.18e-01
alpha_sample_ttz_sys	2.0012e-01	+/- 9.95e-01
alpha_sample_tz_sys	1.6749e-01	+/- 1.00e+00
alpha_sample_wz_sys	1.2732e-01	+/- 9.84e-01
alpha_sample_fakes_sys	4.5030e-01	+/- 7.17e-01
mu	2.4975e+00	+/- 1.29e+01

$\alpha$  values for post fit thg  $k_t=1$

Floating Parameter	FinalValue	+/- Error
Lumi	1.0085e+00	+/- 2.40e-02
alpha_sample_tth_sys	1.9290e-01	+/- 1.00e+00
alpha_sample_ttw_sys	8.7911e-01	+/- 9.42e-01
alpha_sample_ttz_sys	2.0370e-01	+/- 9.94e-01
alpha_sample_tz_sys	1.8269e-01	+/- 9.69e-01
alpha_sample_wz_sys	1.4244e-01	+/- 9.99e-01
alpha_sample_fakes_sys	1.4243e-01	+/- 9.98e-01
mu	6.9361e-02	+/- 1.02e+00

# Results

## Likelihood scan

- Likelihood function (often simply the likelihood) is a function of the parameters of a statistical model, given specific observed data.
- Likelihood functions play a key role in frequentist inference, especially methods of estimating a parameter from a set of statistics.
- In informal contexts, "likelihood" is often used as a synonym for probability.

# Statistical test

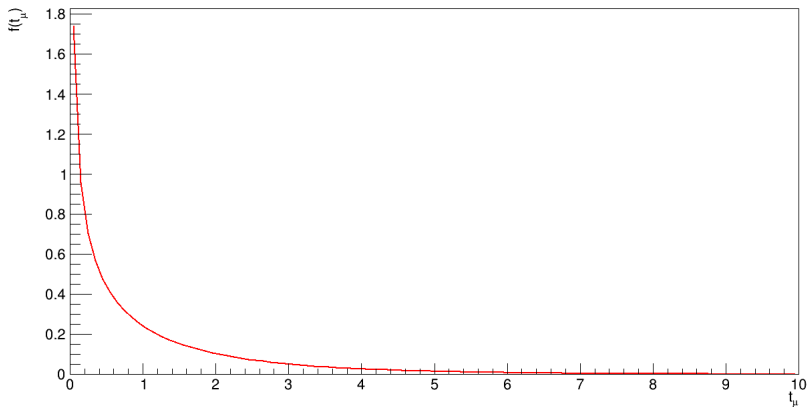
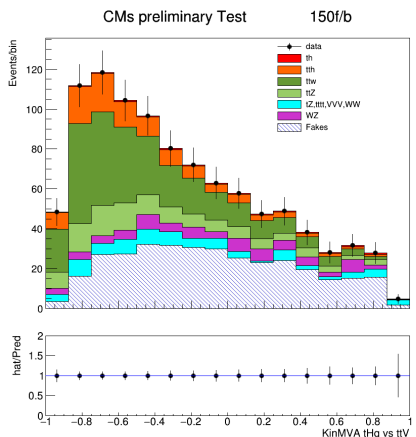


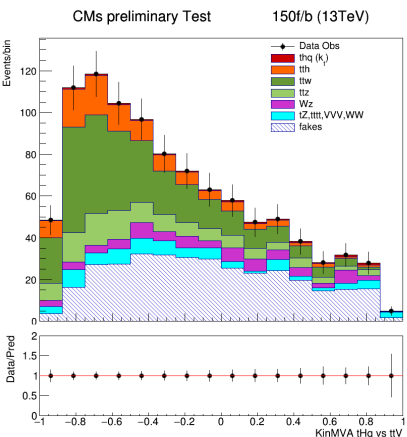
Figure: Statistic test plot  $f(t_\mu)$  vs  $t_\mu$  with  $t_\mu = -2 \ln \lambda(\mu)$

## Luminosity scale

150 fb



## Prefit



## Post fit

## Luminosity scale

150 fb

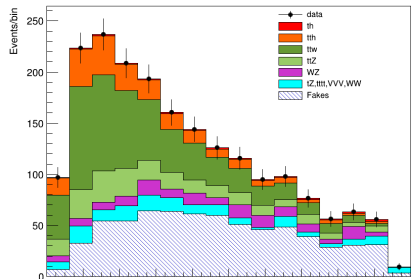
event	N prefit	N Postfit
tH	$8.89972 \pm 0.885511$	$8.89972 \pm 57.2784$
ttH	$101.031 \pm 9.45$	$101.031 \pm 9.27757$
ttW	$284.248 \pm 39.8961$	$284.248 \pm 31.3604$
ttZ	$108.175 \pm 13.3806$	$108.175 \pm 13.1161$
tZ	$71.7409 \pm 34.1567$	$71.7409 \pm 31.8423$
WZ	$67.8134 \pm$	$67.8134 \pm 31.8861$
fakes	$338.189 \pm 170.744$	$338.189 \pm 84.302$

# Luminosity scale

300 fb

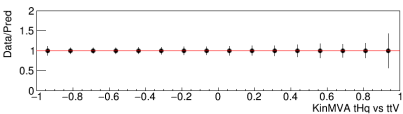
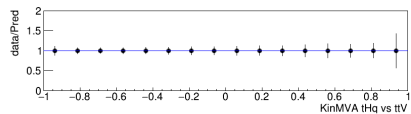
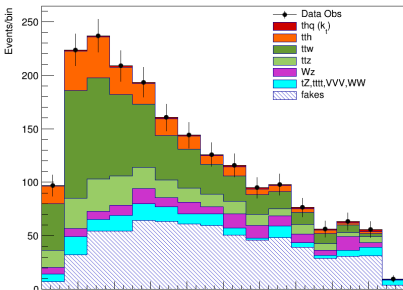
CMs preliminary Test

300f/b



CMs preliminary Test

300f/b



Prefit

post fit

## Luminosity scale

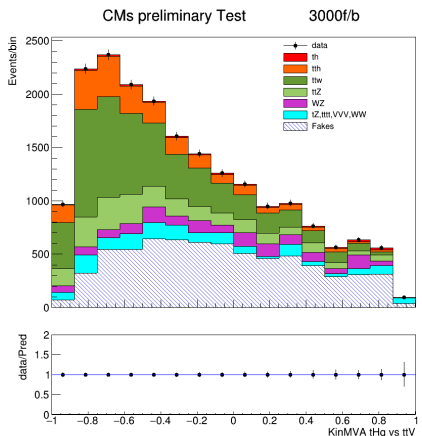
300 fb

## Table of yields for background and signal

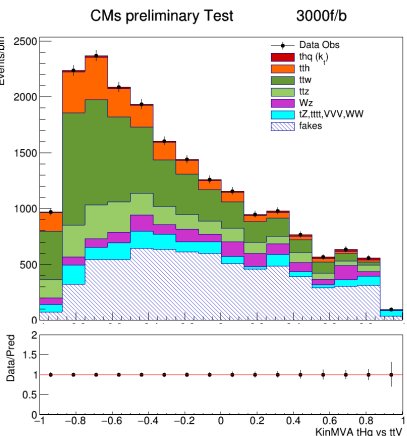
tH	17.7994 $\pm$ 85.9204	17.7994 $\pm$ 85.9204
ttH	202.061 $\pm$ 18.9162	202.061 $\pm$ 18.4728
ttW	568.496 $\pm$ 79.7922	568.496 $\pm$ 56.3133
ttZ	216.351 $\pm$ 26.7611	216.351 $\pm$ 26.099
tZ	143.482 $\pm$ 72.2699	143.482 $\pm$ 58.5044
WZ	135.627 $\pm$ 68.3133	135.627 $\pm$ 60.7892
fakes	676.379 $\pm$ 341.488	676.379 $\pm$ 133.725

## Luminosity scale

3000 fb



## Prefit



## Post fit

## Luminosity scale

3000 fb

## Table of yields for background and signal

event	N prefit	N Postfit
tH	5076.72 $\pm$ 505.128	5076.72 $\pm$ 643.706
ttH	2020.61 $\pm$ 189.162	2020.61 $\pm$ 183.997
ttW	5684.96 $\pm$ 797.922	5684.96 $\pm$ 561.487
ttZ	2163.51 $\pm$ 267.611	2163.51 $\pm$ 256.289
tZ	1434.82 $\pm$ 722.699	1434.82 $\pm$ 303.361
WZ	1356.27 $\pm$ 683.133	1356.27 $\pm$ 383.271
fakes	6763.79 $\pm$ 3414.88	6763.79 $\pm$ 591.597